Structure and dynamics of solitons in a nematic liquid crystal in a rotating magnetic field

Chun Zheng and Robert B. Meyer
The Martin Fisher School of Physics, Brandeis University, Waltham, Massachusetts 02254-9110
(Received 24 March 1997)

We study the structure and speed of movement of dynamic solitons in a thin layer of nematic liquid crystal, with homeotropic boundary conditions, in a rotating magnetic field. Based on numerical integration of the equations of motion, we find that the soliton must be described as a two-dimensional object with unconstrained director motion. From some qualitative features of the soliton structure seen in our numerical results, we are able to deduce an approximate analytic theory of the physics of the soliton structure and dynamics that accounts accurately for the observations. The basic elements of this picture are a tilted plane in which the director rotates as the soliton passes a point, with the tilt angle of the plane being dictated by a second Fréedericksz transition within the soliton. [S1063-651X(97)14910-8]

PACS number(s): 61.30.Gd, 07.05.Tp, 47.54.+r

I. INTRODUCTION

Several experimental studies have been carried out on the dynamical system consisting of a layer of nematic liquid crystal in a continuously rotating magnetic field [1–8]. A general introduction to the phenomenology of this system is presented elsewhere [1,9], along with theoretical analysis of some of the observations [2,3,5]. In this paper, we concentrate on one of the simplest of the observed phenomena, propagating solitary waves. We review just enough of the general system to address this phenomenon, present the simplest one dimensional theoretical description based on the overdamped sine-Gordon equation, compare it to observations, and then present the two-dimensional model of the soliton that we have developed through a combination of numerical simulations and analytic studies.

The basic physical system consists of a thin nematic layer contained between parallel glass plates treated to align the nematic director perpendicular to the plates. A uniform magnetic field is applied, with the field parallel to the plane of the sample. For the purposes of the discussion here, we consider field strengths well above the threshold field for the Fréedericksz transition, so that in a static uniform sample, the director in the sample midplane is parallel to the field. The sample is rotated about an axis normal to its plane, and for high enough fields and low enough rotation rates, the field applies sufficient torque so that the director follows the field synchronously, with a phase lag angle α due to the rotational viscosity of the nematic. A stable, uniform, steady state condition for this system is described by this phase angle being a constant, α_0, at every point in the midplane of the sample. However, if a local disturbance causes the phase angle to increase beyond some critical value, a phase slippage by π radians can occur locally, and the boundary of this region is then a solitary wave, or kink, which propagates away from the source. Dust particles in the sample serve as nucleation sources for a sequence of such solitary wave, or soliton, rings forming a bulls-eye pattern about the nucleation point. Each ring is well separated from its neighbors in the sequence, and propagates as an isolated object. In this paper, we look at a single soliton, in the limit of large radius, so the curvature of the ring has negligible effect on the soliton structure and propagation speed. In the experiments on this system, the main measurable characteristic of a soliton is its propagation speed, which has been studied as a function of magnetic field strength and rotation rate. As shown below, one can calculate this speed from a simple one dimensional model of the soliton. The measurements and calculations disagree in one major way. The calculated speed goes to zero linearly as rotation speed goes to zero, for any magnetic field, while in the observations, the speed drops abruptly to zero at a finite rotation rate, the value of which depends on the magnetic field. We present first the simple model, since it is the basis for later calculations.

We define a local coordinate system, fixed in the sample, in which y is parallel to the soliton, along which the structure is invariant, and x is perpendicular to the soliton, parallel to its direction of propagation. Looking only at the phase lag angle as a function of x in the sample midplane, one can write down an equation of motion for α, involving the elastic, viscous, and field torques on the director. If one is looking explicitly for soliton solutions, which propagate with a fixed shape and speed v, one can use a coordinate proportional to $x-vt$. This model of the soliton is governed by the overdamped sine-Gordon equation [1]

$$\frac{\partial^2\alpha}{\partial\xi^2}+2\frac{v}{v_0}\frac{\partial\alpha}{\partial\xi}-\frac{1}{2}\sin 2\alpha+\frac{1}{2}\omega\tau=0, \tag{1}$$

where ω is the angular velocity of the rotating magnetic field, τ the magnetic response time constant, and v_0 a reference velocity. The coordinate $\xi=(x-vt)/\xi_h$. The parameters defined here are expressed as

$$\tau=\frac{2\gamma_1}{\chi_a H^2}, \tag{2}$$

$$v_0=4\xi_h/\tau=2H\sqrt{K\chi_a}/\gamma_1, \tag{3}$$

$$\xi_h=\sqrt{K/\chi_a}/H. \tag{4}$$

Here H is the magnetic field strength, γ_1 the nematic rotational viscosity, χ_a the anisotropy of the magnetic suscepti-

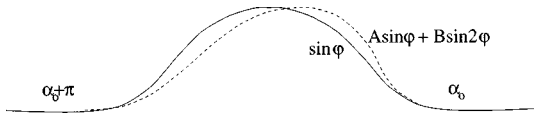

FIG. 1. A spatial plot of $-\partial\alpha/\partial\xi$. The static solution of the sine-Gordon equation is spatially symmetric. The structure of a dynamic soliton, however, is asymmetric.

bility, and K the nematic curvature elastic constant. We have assumed for now that all three elastic constants are equal. ξ_h is the magnetic coherence length.

A soliton solution of Eq. (1) corresponds to the change of α in the range $[\alpha_0, \alpha_0+\pi]$, where α_0 is the phase lag in the uniform region ahead of the soliton and determined by

$$\sin 2\alpha_0 = \omega\tau. \tag{5}$$

Changing variable α to $\varphi=\alpha-\alpha_0$, Eq. (1) can be rewritten in another form:

$$\frac{\partial^2\varphi}{\partial\xi^2}+2\frac{v}{v_0}\frac{\partial\varphi}{\partial\xi}+\sin\alpha_0\cos\alpha_0(1-\cos 2\varphi)$$

$$-\frac{1}{2}(\cos^2\alpha_0-\sin^2\alpha_0)\sin 2\varphi=0. \tag{6}$$

Although there is no analytic solution for the sine-Gordon equation, we can obtain an approximate solution for the speed of a soliton using a perturbation technique. For $v=0$ and $\omega=0$ (hence $\alpha_0=0$), Eq. (1) has a solution of the form

$$\frac{\partial\alpha}{\partial\xi}=-\sin\alpha. \tag{7}$$

This corresponds to a static soliton.

Assuming that the structure of a dynamic soliton is only a perturbation of the static one, we take the trial solution

$$\frac{\partial\alpha}{\partial\xi}=-A\sin(\alpha-\alpha_0)-B\sin 2(\alpha-\alpha_0). \tag{8}$$

This satisfies the requirement that when $\alpha=\alpha_0$ or $\alpha=\alpha_0+\pi$, $\partial\alpha/\partial\xi=0$ (Fig. 1) and that α approaches its asymptotic values exponentially on both sides of the soliton.

Expanding equation (1) with ansatz (8) near both $\alpha=\alpha_0$ and $\alpha=\alpha_0+\pi$ and demanding that v be independent of α, we have

$$A=\sqrt{\left(\frac{v}{v_0}\right)^2+\sqrt{1-(\omega\tau)^2}},\quad B=\frac{1}{2}\frac{v}{v_0}. \tag{9}$$

Notice that Eq. (1) is the equation of motion of a particle in a viscous medium and a conservative potential if one thinks of (α,ξ) as (position, time). The potential has a mean slope and a series of hills. The soliton solution corresponds to the motion of a particle starting from one local potential maximum with 0 velocity and sliding down to the next maximum where it just comes to rest due to friction. The conservation of energy for this trajectory, converting potential energy to friction losses, requires that

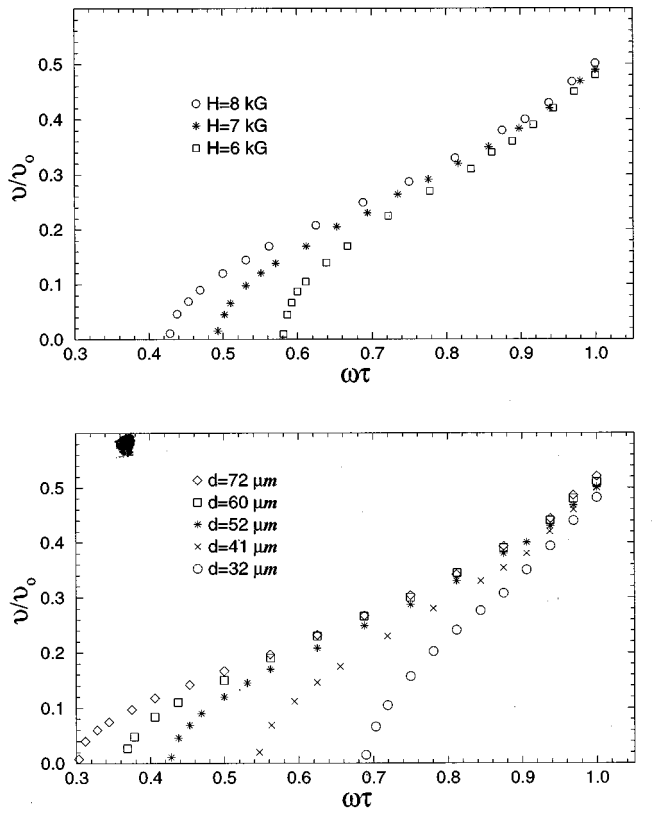

FIG. 2. Velocity of dynamic solitons from numerical simulation. Top: $d=52$ μm. Bottom: $H=8$ kG.

$$\int_{\alpha_0}^{\alpha_0+\pi}\frac{1}{2}\omega\tau\,d\alpha=\int_{\alpha_0}^{\alpha_0+\pi}2\frac{v}{v_0}\frac{\partial\alpha}{\partial\xi}d\alpha. \tag{10}$$

Combined with Eq. (8) this gives an expression for A, which, when combined with Eq. (9), leads to an analytic expression for the velocity:

$$2(v/v_0)^2=\sqrt{1-(\omega\tau)^2+(\omega\tau\pi/4)^2}-\sqrt{1-(\omega\tau)^2}. \tag{11}$$

This approximate solution for the speed of a soliton from the overdamped sine-Gordon equation agrees with precise numerical results [10] to within a few percent in the whole range of $\omega\tau$ from 0 to 1. The speed varies linearly with $\omega\tau$, with the correct slope near $\omega\tau=0$, and has a weak vertical slope singularity at $\omega\tau=1$, which appears to be correct. However, as we indicated before, this answer does not agree with experiments. For comparison of theory with data, see Fig. 2 of Ref. [1]. The most significant discrepancy is that this formula predicts the speed of a soliton to go smoothly to 0 only as $\omega\tau$ approaches 0, while in experiments the transition of a dynamic soliton to a static one occurs abruptly at a finite $\omega\tau$.

An initial idea considered qualitatively by Migler and Meyer to explain the transition from dynamic to static behavior was that in the dynamic soliton the director stays parallel to the sample plane during soliton motion, while in the static soliton, the director is oriented vertically, i.e., normal to the sample plane, in the center of the soliton. This structural transition was viewed as being driven by torques from the sample surfaces, at which the director is vertical,

and as being associated with slow soliton speed, allowing enough time for the director to reorient from in-plane to vertical as the soliton passed a point in the sample. However, no quantitative model emerged from this idea.

Gilli *et al.* and Frisch *et al.* [4,5] developed theory and carried out experiments on a closely related system, differing from ours in that there is only weak tilting of the director from the vertical over the whole sample. The role of director tilting within the soliton in the dynamic to static transition was analyzed in terms of Ising and Bloch wall structures. They were able to develop theory in terms of the small in-plane component of the director, as a two component order parameter, for which the equation of motion is a time dependent Ginzburg-Landau equation. For this system, they could calculate the critical condition for the static to dynamic transition, and the speed of the dynamic solitons. We were, however, forced to consider arbitrarily large director tilts, and unconstrained director motion.

We wanted to explore the role of director orientation and surface torques in soliton speed, and also to seek explanations to some other unusual soliton behavior reported previously [11], such as solitons colliding without annihilating. We therefore developed a two dimensional model for unconstrained director motion, still assuming that the soliton structure was invariant along its length. Our numerical simulations described below gave results strikingly similar to the experiments. These led us to new insights into the soliton structure, and a clear physical model of the soliton dynamics, along with an approximate analytic calculation of soliton velocity.

II. TWO-DIMENSIONAL MODEL WITH θ-α COUPLING

The general equations of motion for the nematic director can be derived in different ways [12,13]. In the simplest (one-K) model where all three elastic constants are equal and flow effects are ignored, we have a torque equation

$$\gamma_1 \frac{\partial n_\mu}{\partial t} = K\nabla^2 n_\mu + \chi_a n_\nu H_\nu H_\mu , \tag{12}$$

with the constraint of $n_\mu n_\mu = 1$, where $\mu,\nu = x,y,z$ and the Einstein summation convention is adopted. Here we denote the local director $\mathbf{n}$ with its components n_μ.

The influence of flow upon the movement of solitons can be shown to be rather small [14]. The anisotropy in elasticity, however, is an important factor in determining the behavior of dynamic solitons. In the next section we allow K_2 to be different from K_1 and K_3 and study how the behavior of a dynamic soliton changes. Letting $K_1 = K_3 = K$ and $K_2/K = \lambda$, Eq. (12) is modified with an extra term Δ on the right-hand side, which is given by

$$\Delta = (1-\lambda)K[C\ \mathrm{curl}\mathbf{n} + \mathrm{curl}(C\mathbf{n})], \tag{13}$$

where $C = \mathbf{n}\cdot\mathrm{curl}\mathbf{n}$ [12].

We have solved the above equations numerically in a two dimensional grid in the x-z plane where x is the direction of the soliton movement and z is the rotation axis of the magnetic field, which is perpendicular to the surfaces of the sample. As described in [1], the initial alignment of the liquid crystal material sandwiched between two glass plates is homeotropic, that is, the director is perpendicular to the surfaces. The soliton itself lies along the invariant direction y. The parameters used in our simulation are (in cgs units) $\gamma_1 = 0.5$ P, $K = 3.0\times10^{-7}$ dyn, and $\chi_a = 0.5\times10^{-7}$.

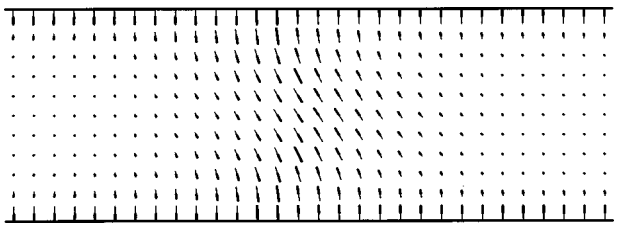

FIG. 3. A snapshot of the director profile in the x-z plane from our computer simulation (one-K model). $d = 52$ μm, $H = 8$ kG, $\omega = 1.45$ s^{-1}.

Using rescaled velocity v/v_0 and normalized angular velocity of the magnetic field $\omega' = \omega\tau$, the speeds of solitons for different sample thicknesses and different magnetic fields are presented in Fig. 2. There are several points to be noted: (1) both the thickness of the sample and the strength of magnetic field affect the speed of a soliton. However, when $\omega' \to 1$, the speeds of solitons converge toward a uniform curve; (2) when $\omega' \to 1$, the speed of a soliton does not exhibit a vertical slope singularity as predicted by the sine-Gordon equation; (3) the speed of a soliton goes continuously to 0 at a finite ω'. As will be shown later, this critical value ω_c' has a well defined meaning.

A typical snapshot of the cross section of a soliton is shown in Fig. 3. Notice the essential feature that the director is not parallel to the sample plane in the middle of the soliton, but rather is tilted at some oblique angle. Far from the center of the soliton the director is parallel to the sample plane, because the magnetic field is high above the threshold for the Fréedericksz transition. Thus, two angles as functions of both x and z are needed to describe the soliton. The second angle is the polar angle θ between the z axis and the director.

To keep the resulting model simple we adopt the following approximate method: first, we derive the coupled equations for θ and α in only one dimension (x), ignoring z. Based on another feature seen in our numerical results, this set of two equations is transformed into a single equation with two new variables, θ_0 and β, in which θ_0 is independent of x. Then we consider the z dependence of the director and solve for θ_0, while β is kept independent of z. Thus we have decoupled the 2 degrees of freedom from the two dimensionality and each degree of freedom can be solved for separately. This approximation captures the basic physics of the problem with the simplest equations.

We first consider the θ-α coupling as a function of x. Letting θ be the polar angle of a local director, and assuming that both θ and α are independent of z, we have

$$\frac{\partial^2\theta}{\partial\xi^2} + 2\frac{v}{v_0}\frac{\partial\theta}{\partial\xi} + \frac{1}{2}\left[\cos^2\alpha - \left(\frac{\partial\alpha}{\partial\xi}\right)^2\right]\sin 2\theta = 0,$$

$$\frac{\partial^2\alpha}{\partial\xi^2} + 2\left(\frac{v}{v_0} + \frac{\cos\theta}{\sin\theta}\frac{\partial\theta}{\partial\xi}\right)\frac{\partial\alpha}{\partial\xi} - \frac{1}{2}\sin 2\alpha + \frac{1}{2}\omega\tau = 0. \tag{14}$$

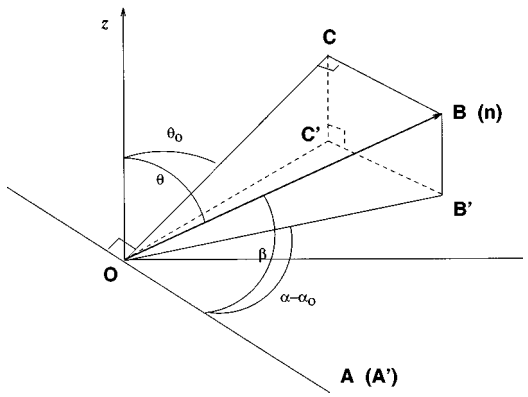

FIG. 4. The soliton plane, or β plane, in which the director rotates, is the OBC plane, tilted by polar angle θ_0. $OB'C'$ is the x-y plane. The director (parallel to OB) is located by phase angle β in the soliton plane, and projects to angle $\alpha-\alpha_0$ on the x-y plane. Far from the soliton, the director is parallel to the line $OA(A')$, which is common to the soliton plane and the x-y plane. OC and OC' are perpendicular to OA.

The difficulty in solving the coupled equations (14) comes from the singularity in $\partial\alpha/\partial\xi$ when a dynamic soliton goes to the static limit. It turns out that in that limit, at the center of the soliton θ is 0 and $\partial\alpha/\partial\xi$ is no longer defined. To avoid this problem, we make the following transformation of variables, inspired by our computer simulation results.

Figure 3 is a snapshot of the director profile at the instant when in the uniform bulk the director is aligned perpendicular to the page in the sample midplane. From this picture one can visualize a set of planes that are perpendicular to the paper surface at this instant, and parallel to the director in the middle of the soliton. Along the x direction, in the midplane, the director can be seen as lying parallel to this series of parallel planes, and as the field rotates, the planes and director rotate together. The set of planes make a constant polar angle θ_0 with the z axis. θ_0 is a function only of z, being maximum at the midplane of the sample and zero on the surfaces. In the new coordinate system (Fig. 4) we specify the local director by the angles θ_0 and β, which is the projection of α-α_0 onto the tilted soliton plane. The relationship between (θ,α) and (θ_o,β) is

$$\sin\theta\cos(\alpha-\alpha_0)=\cos\beta,$$

$$\cos\theta=\cos\theta_0\sin\beta. \tag{15}$$

Using Eq. (15), Eq. (14) can be transformed into

$$\frac{\partial^2\beta}{\partial\xi^2}+2\frac{v}{v_0}\frac{\partial\beta}{\partial\xi}+\sin\theta_0\sin\alpha_0\cos\alpha_0(1-\cos2\beta)$$

$$-\frac{1}{2}(\cos^2\alpha_0-\sin^2\theta_0\sin^2\alpha_0)\sin2\beta=0. \tag{16}$$

This equation is very similar to Eq. (6). When θ_0 is $\pi/2$, they are identical. When θ_0 is 0, however, Eq. (16) is equivalent to Eq. (6) when α_0 is set to 0, which is a static soliton equation with 0 velocity. [Setting α_0 to 0 is equivalent to setting $\omega\tau$ to 0. See Eqs. (5) and (11)]. It is clear that the speed of a soliton is dependent on the angle θ_0. Using again the perturbation solution for the sine-Gordon equation, we find the speed of a soliton corresponding to Eq. (16) to be

$$2(v/v_0)^2=\sqrt{(\cos^2\alpha_0-\sin^2\theta_0\sin^2\alpha_0)^2+[(\pi/4)\sin\theta_0\sin2\alpha_0]^2}-(\cos^2\alpha_0-\sin^2\theta_0\sin^2\alpha_0). \tag{17}$$

For small θ_0 the velocity increases linearly with θ_0, and it increases monotonically as θ_0 increases from 0 to $\pi/2$. Comparing this result with the work of Coullet *et al.* [15] on chirality breaking transitions in domain walls, what we have done is to find an explicit description of the soliton in terms of a phase angle β and the ''chiral order parameter'' θ_0.

Although θ_0 is independent of x, it varies with z. It is zero on the surfaces, and reaches a maximum value θ_m at the midplane of the sample. Since the soliton moves as a whole, we can take the maximum value θ_m for θ_0 and expect Eq. (17) to give an upper limit for the speed of a dynamic soliton. A more accurate model would include the z variation in the initial equations, but our approach allows us to reach a simple analytic approximate expression for the velocity. What remains to be done in this approximate model is to understand how $\theta_0(z)$, or more simply θ_m, depends on field strength, rotation rate, and sample thickness. This will allow us to understand why the soliton speed varies so much from the sine-Gordon model.

To determine the value of θ_m, one has to consider the coupling of the director field to the z dimension. We have discovered that the dependence of $\theta_0(z)$ on other parameters can be understood as a second Fréedericksz transition at the center of a soliton.

For a static soliton (a domain wall) in a nonrotating field, in the one elastic constant approximation, in an infinite sample with no boundaries to exert torques, the director can rotate about any axis perpendicular to the magnetic field in going from one side of the soliton to the other, since the elastic energy is independent of rotation axis. In terms of our coordinate system, if the director remains parallel to the sample plane, the elastic distortion in the wall is all splay bend, while if it rotates parallel to the vertical plane, it is splay-bend or twist, depending on the orientation of the director far from the wall. However, in our finite sample with homeotropic boundary conditions, the vertical orientation is energetically favored, since this is compatible with the vertical director at the boundaries. At low rotation rates, the director in the soliton remains parallel to the vertical plane, the soliton is symmetric about its center, and the soliton velocity is zero.

As the rotation rate increases, and the angle α_0 increases, there is an increasingly large component of the magnetic

TABLE I. Comparison of prediction by Eq. (20) and numerical results for the critical value of $\omega\tau$ for the dynamic to static soliton transition.

H/H_c	7.49	5.41	4.05
$(\omega\tau)_c$ theory	0.26	0.36	0.48
$(\omega\tau)_c$ numerical	0.30	0.43	0.58

field, $H\sin\alpha_0$, perpendicular to the vertical plane to which the director in the soliton is parallel. At some critical rotation rate, the torque due to this perpendicular field component causes a second Fréedericksz transition, in which the director in the middle of the soliton starts to tilt away from vertical. This breaks the symmetry of the soliton, and causes it to begin to move. The director can tilt in two degenerate directions, so a single static soliton can break into segments that propagate in opposite directions while still being held together where they meet, generating spiral patterns [3–5]. These changes in structure and symmetry of the soliton when it becomes dynamic have been described in the cited works, and analyzed in the limit of small global director tilt [4,5]; now we can account for the phase transition and velocity of the soliton in the general case of large director tilt.

If we simply use the classic Fréedericksz transition in a uniform sample for our model of the transition in the soliton, then we can calculate the critical value of α_0, or equivalently of $\omega\tau$, and the dependence of $\theta_0(z)$ and θ_m on the other variables in the problem. In this case, $\theta_0(z)$ can be expressed as an elliptic integral, and we have [16] an implicit relation between θ_m and α_0:

$$H\sin\alpha_0 = H_c \frac{2}{\pi}\int_0^{\theta_m} \frac{d\theta_0}{\sqrt{\sin^2\theta_m - \sin^2\theta_0}}, \tag{18}$$

in which $H_c = (\pi/d)\sqrt{K/\chi_a}$.

When $\theta_m \to 0$, this equation gives a critical value of α_0, or, equivalently, of $\omega\tau$ for the dynamic to static soliton transition:

$$\sin\alpha_c = \frac{H_c}{H}. \tag{19}$$

Since $\omega\tau = \sin 2\alpha_0 = 2\sin\alpha_0\cos\alpha_0$, we have

$$(\omega\tau)_c = 2\frac{H_c}{H}\sqrt{1-\left(\frac{H_c}{H}\right)^2}. \tag{20}$$

We have compared this prediction for the soliton transition with our numerical results in Table I. They tend to agree for large values of H/H_c. The smaller the value of H/H_c, the less accurate the prediction.

To account for this difference, one of our first ideas was that in the dynamic soliton the angle θ_0 at a given location might not have time to change as the soliton moved past that point; this would favor the director simply staying parallel to the sample plane ($\theta_0 = \pi/2$). To test this idea, we compared the characteristic time for the director to respond to the magnetic field τ to the time of passage of a soliton, $t_h \simeq 2\xi_h/v$. With the material constants we used in our simulations, at the maximum velocity, t_h is about 5 times larger than τ. This means the soliton motion is a relatively slow process, with ample time for θ_0 to reach quasistatic equilibrium.

TABLE II. Comparison of theory and numerical data on the critical value of $\omega\tau$ for the dynamic to static soliton transition.

d (μm)	H (kG)	H/H_c	$(\omega\tau)_c$ Theory	$(\omega\tau)_c$ Numerical
32	8	3.33	0.71	0.69
41	8	4.26	0.55	0.55
41	9	4.80	0.49	0.49
52	6	4.05	0.58	0.58
52	7	4.73	0.49	0.49
52	8	5.41	0.43	0.43
60	8	6.24	0.36	0.36
72	8	7.49	0.30	0.30

It is clear that the internal structure of the soliton is quite different from a translationally invariant sample, so our simple estimate for the Fréedericksz transition may be poor. However, just what elements of the internal structure, static or dynamic, affect the critical condition for tilting of the soliton plane is less clear. The data indicate that the transition takes place at higher values of $\omega\tau$ than calculated from Eq. (20). This can be expressed as a larger value for H_c for the transition in the soliton, or as a different projection angle for the magnetic field, larger than the value of α_c calculated above, by a small correction angle δ. By looking at our data, we found that this angle can be expressed as $\delta = (H_c/H)^2$. Rewriting Eq. (5) with this added term, and using α_c from Eq. (19), we have $\omega\tau = \sin 2(\alpha_c + \delta)$, or,

$$(\omega\tau)_c = \sin 2\left[\arcsin\left(\frac{H_c}{H}\right) + \left(\frac{H_c}{H}\right)^2\right]. \tag{21}$$

As seen in Table II, this accurately describes the transition from static to dynamic solitons for a large range of fields and sample thicknesses. For a typical value of $H/H_c = 5$, $\delta = 0.04$ rad, a small correction. If we assume that δ is a constant independent of ω, then above the critical value of $\omega\tau$ one can calculate the maximum tilt angle θ_m as a function of $\omega\tau$ from the implicit relationship

$$\sin\left[\frac{1}{2}\arcsin(\omega\tau) - \left(\frac{H_c}{H}\right)^2\right] = \frac{2}{\pi}\frac{H_c}{H}\int_0^{\theta_m}\frac{d\theta}{\sqrt{\sin^2\theta_m - \sin^2\theta}}. \tag{22}$$

In Fig. 5 we have plotted the calculated values of θ_m versus $\omega\tau$ and made a comparison with our numerical data. It can be seen from the graph that the behavior of θ_m is very close to what is expected for a Fréedericksz transition. Finally, we can use these results for θ_m to calculate the speed of the dynamic soliton from Eq. (17). We choose an example of $d = 72$ μm and $H = 8$ kG. The comparison of theory with the numerical data is shown in Fig. 6. As expected, the pre-

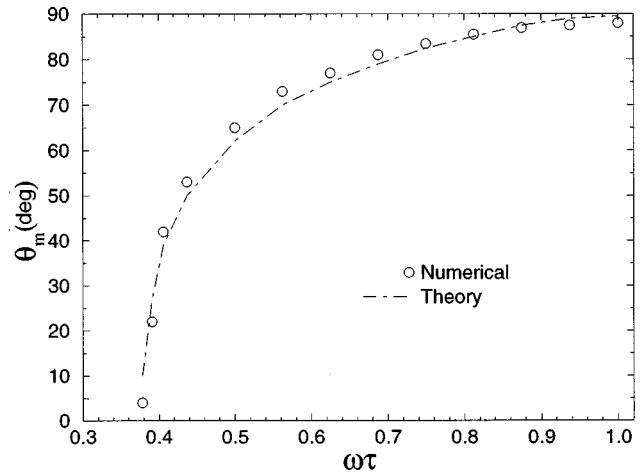

FIG. 5. The comparison of theory and numerical results for the relationship between θ_m and $\omega\tau$. The theory curve is from Eq. (22). $H/H_c = 6.24$.

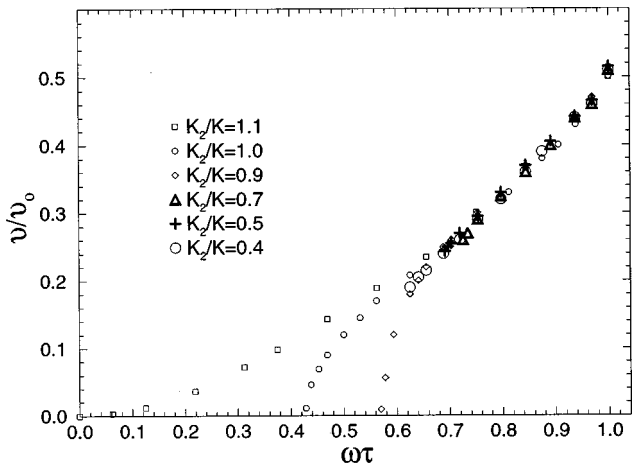

FIG. 7. When K_2/K is below a certain limit (~ 0.7), the velocity of a soliton drops discontinuously and the transition from dynamic to static becomes first order. $d = 52$ μm, $H = 8$ kG.

diction by our theory is above the numerical data, since we used the angle θ_m, which is the maximum value of θ_0 in Eq. (17).

The qualitative functional form of soliton speed versus $\omega\tau$ shown in Fig. 6 compares well to the data measured by Nasuno *et al.* [6]. Their data show a continuous decrease in velocity of the dynamic soliton in the transition to a static soliton, quite different from the discontinuous transition with hysteresis found by Migler and Meyer [1]. Although Nasuno *et al.* compare their data to the predictions of a second order transition for the small global director tilt limit presented by Gilli *et al.* and Frisch *et al.* [4,5], in fact their experimental conditions ($H/H_c = 3.8$) are in the regime of large director tilt, the same as Migler and Meyer's. We have found that the seeming discrepancy between experiments can be explained by the role of the twist elastic constant K_2 in changing the nature of the soltion transition.

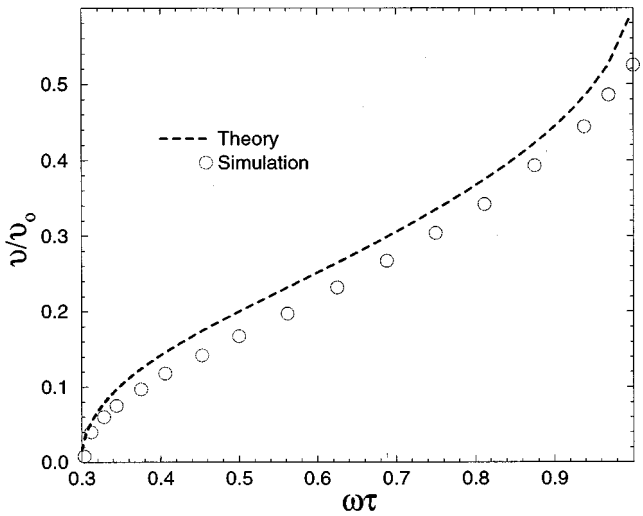

FIG. 6. The theoretical prediction of the speed of solitons is slightly above the numerical simulation results.

III. EFFECTS OF VARYING K_2/K

The effect of varying elastic constant K_2 on the movement of a dynamic soliton is shown in Fig. 7. This is a rather complicated situation. When the three elastic constants are not equal, the propagating object is no longer strictly a soliton, since it oscillates in its shape and speed. When K_2 is not too small ($K_2/K \simeq 0.7-1.0$ for $d = 52$ μm, $H = 8$ kG), the average speed of a dynamic soliton behaves similarly to that of the one-K model. It goes continuously to zero, and this zero point shifts toward larger ω' as K_2 becomes smaller. When K_2 is considerably smaller than K ($K_2/K \leqslant 0.7$), a dynamic soliton's speed drops to zero from a finite value; the transition from a dynamic soliton to a static one becomes first order. There is also a hysteresis loop associated with this point. This is the case observed in Migler's experiments [1]. When K_2 becomes even smaller, the first order transition point shifts back toward lower ω', with larger hysteresis.

Our interpretation of these phenomena involves several points. First, small K_2 favors the static soliton energetically, since it spends half its time as a twist structure, compared to the dynamic soliton, which is pure splay bend for $\theta_0 = \pi/2$. This moves the transition to higher values of $\omega\tau$. Explaining the change to a first order transition involves understanding the initial distortion of the soliton structure at small θ_0; if the initial replacement of twist curvature by bend curvature raises the soliton energy by more than the reduction of field energy due to the tilt, then small tilts are disfavored, while large tilts may still lower the total enregy. This results in a first order transition.

At high fields, more complex changes in the soliton structure take place. As seen in Fig. 8 there is a remarkable distortion of the previously simple soliton structure. With K_2 small, and θ_m near $\pi/2$, the elastic coupling in the z direction is weak, and the soliton can easily be deformed. The high tilt region in the midplane tends to move faster than the low tilt parts near the surfaces, resulting in the stretched structure seen in Fig. 8. In this stretched structure, the leading edge is more subject to the influence of the bulk, which forces the soliton to stay in the x-y plane. Thus this stretching may

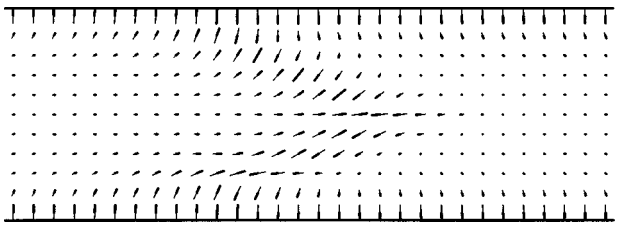

FIG. 8. When K_2 is substantially smaller than K (here $K_2/K=0.5$), at high fields the structure of a soliton is dramatically different from the one-K model. ($d=52$ μm, $H=8$ kG, $\omega=2.23$ s^{-1}.)

have a stabilizing effect, leading to increased hysteresis in the soliton transition.

In Fig. 7 we have also shown a case where K_2 is bigger than K. Although this is an artificial case, it has an interesting consequence. A bigger K_2 means we have made the static soliton less stable energetically, relative to the dynamic one. Remarkably, a small increase in K_2 pushes the transition point to $\omega\tau=0$. The behavior of a soliton in this case resembles more the prediction of the sine-Gordon equation. Notice, however, that there is still tilting of the director in the soliton, and the qualitative dependence of speed on tilt angle is still valid. Figure 9 is a plot of θ_m versus $\omega\tau$. Notice that the tilt angle still goes continuously to zero, now at $\omega\tau=0$, and linearly, not with vertical slope. This results in the speed varying quadratically with low values of $\omega\tau$.

Finally, we return to the discrepency between the results of Refs. [1] and [6] on the order of the soliton transition. The two groups used different materials, but with similar values of K_2/K. However, Nasuno *et al.* used a rather low magnetic field ($H/H_c=3.8$) compared to Migler and Mayer ($H/H_c=6.8$) We have found that the relative value of K_2 at which the transition changes from second to first order depends on magnetic field, with low fields favoring a second order transition for a larger range of K_2. In fact, we ran our simulation for conditions as close as possible to those used by Nasuno *et al.* using a value of $K_2/K=0.5$, a reasonable estimate for their material, MBBA. We still found a first order transition. However, for a somewhat lower field ($H/H_c=3.33$) the transition was again second order. The precise location of the tricritical point separating first and second order transitions may also depend on the difference between K_1 and K_3, which is large in MBBA, and which we do not account for in our calculations. We conclude that the different results obtained by the two groups are well within the normal range expected, and do not represent a real disargeement. Unfortunately, neither group discovered the change from first order to second order transition with varying field strength that our calculations indicate should exist.

IV. DISCUSSION

We have established a simple model to study the structure and movement of a dynamic soliton. The dynamic soliton is quite different from a static one in structure. It is basically a two dimensional object with 2 degrees of freedom. Our results on the soltion transition and velocity are consistent with experiments and with the previous conclusions of Refs. [4] and [5].

For the one elastic constant limit, our simplified analytic

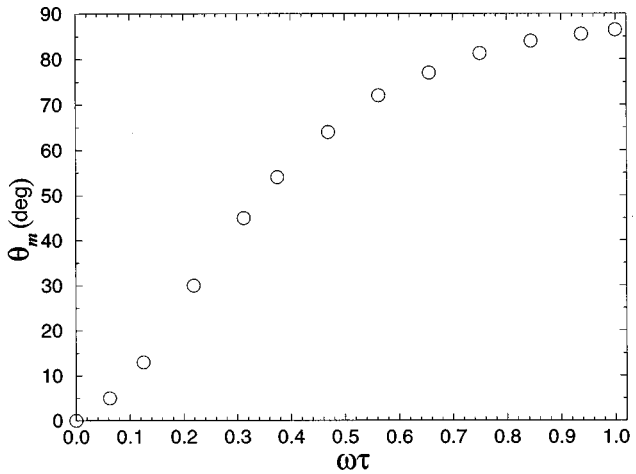

FIG. 9. The tilting angle θ_0 for K_2 larger than K. It is well coordinated with the speed of a soliton.

model based on the numerical simulations shows that to a good degree of approximation, the 2 degrees of freedom can be decoupled, with each being mainly a function of one dimension. The z coupling of the director field can be described by a planar structure, and the tilting of the soliton plane is essential in determining soliton velocity. Moreover, the tilt behavior of the soliton plane can be understood in terms of a quasistatic second Fréedericksz transition inside the soliton, rather than mainly as a dynamic effect. Even for the case of $K_2\neq K$, the dependence of speed on tilt angle seems qualitatively valid.

There are many unanswered questions. The sometimes complex structure of the dynamic soliton in the case of $K_2\leqslant K$, and the first order transition from dynamic to static are far from being explained in any detail. For the one-K approximation, the dependance of the critical point for the dynamic to static soliton transition on magnetic field strength and sample thickness is qualitatively well understood in terms of a second Fréedericksz transition, but the quantitative calculation of the critical point is not complete. Our empirical expression for a correction angle $\delta=(H_c/H)^2$ is not clearly tied to a precise or unique physical argument. One idea is that although the second Fréedericksz transition is quasistatic, there is still a small dynamic correction connected with the asymmetry in the soliton that appears as soon as it starts to move. This could lead to the maximum torque on the β plane occurring for a projection angle not normal to its initial vertical orientation, but off normal by a correction angle δ, proportional to the ratio of field response times $\tau/\tau_c=(H_c/H)^2$. This was the idea that led us to the form for the correction angle we proposed above. However, we have not been able to make the argument more quantitative. Another interpretation is that the internal structure of the soliton results in a critical field component for tilting, H_{cs}, which happens to be larger than H_c. If it also happens that we can write this new critical field as $H_{cs}/H=H_c/H+(H_c/H)^2$, by referring to Eqs. (18)–(22), in the limit of small H_c/H, we can get essentially the same correction angle δ, now representing the larger projection of H normal to the initially vertical β plane, rather than projection of H onto a different direction. However, in this case, we cannot explain the particular form for H_{cs}, or even why it should be larger than H_c.

On the experimental side, in light of our simulation results, it would be interesting to look for the tricritical point in the dynamic to static soliton transition, by a more complete study of soliton speed as a function of magnetic field and rotation rate.

ACKNOWLEDGMENTS

This research was supported by the NSF through Grant No. DMR-9415656, and by the Martin Fisher School of Physics at Brandeis University.

[1] K. B. Migler and R. B. Meyer, Phys. Rev. Lett. **66**, 1485 (1991).
[2] K. B. Migler and R. B. Meyer, Phys. Rev. E **48**, 1218 (1993).
[3] K. B. Migler and R. B. Meyer, Physica D **71**, 412 (1994).
[4] J. M. Gilli, M. Morabito, and T. Frisch, J. Phys. II **4**, 319 (1994).
[5] T. Frisch, P. Coullet, S. Rica, and J. M. Gilli, Phys. Rev. Lett. **72**, 1471 (1994).
[6] S. Nasuno, N. Yoshimo, and S. Kai, Phys. Rev. E **51**, 1598 (1995).
[7] M. Grigutsch and R. Stannarius (unpublished).
[8] E. Pashkovsky *et al.* (unpublished).
[9] *Solitons in Liquid Crystals*, edited by Lui Lam and Jacques Prost (Springer-Verlag, New York, 1992).
[10] M. Buttiker and R. Landauer, Phys. Rev. A **23**, 1397 (1981).
[11] Chun Zheng and R. B. Meyer, Phys. Rev. E **55**, 2882 (1997).
[12] P. G. de Gennes, *The Physics of Liquid Crystals* (Claredon Press, Oxford, 1974).
[13] G. Vertogen and W. H. de Jeu, *Thermotropic Liquid Crystals, Fundamentals* (Springer-Verlag, Berlin, 1988).
[14] C. Zheng and R. B. Meyer (unpublished).
[15] P. Coullet, J. Lega, B. Houchmanzadeh, and J. Lajzerowicz, Phys. Rev. Lett. **65**, 1352 (1990).
[16] Lev M. Blinov, *Electro-Optical and Magneto-Optical Properties of Liquid Crystals* (John Wiley & Sons, New York, 1983).